

Witnessing Entanglement with Second-Order Interference

Magdalena Stobińska*

Instytut Fizyki Teoretycznej, Uniwersytet Warszawski, Warszawa 00-681, Poland

Krzysztof Wódkiewicz†

*Instytut Fizyki Teoretycznej, Uniwersytet Warszawski, Warszawa 00-681, Poland and
Department of Physics and Astronomy, University of New Mexico, Albuquerque, NM 87131-1156, USA*

(Dated: December 3, 2018)

Second-order interference and Hanbury-Brown and Twiss type experiments can provide an operational framework for the construction of witness operators that can test classical and nonclassical properties of a Gaussian squeezed state (GSS), and provide entanglement witness operators to study the separability properties of correlated Gaussian squeezed states.

I. INTRODUCTION

Two-party systems described by Gaussian states play an important role in quantum information [1], continuous-variables (CV) teleportation [2] and CV entanglement [3]. Such states provide physical realizations of entangled CV resources, required to transmit quantum information in highly efficient quantum channels. The general theory of quantum separability for quantum Gaussian squeezed states has been established recently in several papers [4].

In most theoretical applications squeezed two-mode Gaussian states [5] have been used as a physical realization of the original Einstein Podolsky Rosen (EPR) correlated wave function [6]. Such Gaussian squeezed states can be generated in nonlinear optical parametric amplifiers or in four-wave-mixing processes [7]. Recently an efficient method used the Kerr nonlinearity in optical fibers to generate squeezed entanglement in various variables, like phase and amplitude [8], polarization [9] and photon-number [10].

This experimental progress has stimulated various theoretical tools of diagnostics of CV states which can provide a measure of entanglement and squeezing of such states. So far we know that entanglement of such CV states can be tested using the Heisenberg uncertainty relations [11], the partial positivity transposition (PPT) criterion [12], the interference and particle counting [13], or using quantum witness operators [14].

In this paper, we propose to employ the Hanbury-Brown and Twiss (HBT) interference to witness the quantum nature of one-mode squeezed states and the quantum entanglement of two-mode Gaussian squeezed states. This method seems to be rather easy experimentally realizable measuring second-order correlation function of light. We show that using HBT interference one can witness: classical and nonclassical properties of single mode Gaussian squeezed states and test quantum fea-

tures of two-mode uncorrelated squeezed states. With the help of HBT witness operator we study the entanglement of a general EPR states obtained as a nonlocal action of the beam splitter on two input squeezed states. This witness operator is closely related to the HBT interference.

This paper is organized as follows: section II is devoted to a review of well known properties of one-mode Gaussian squeezed state (GSS). The fundamental properties of such state are derived. The P -representability condition is analyzed using a single mode quantum witness operator. Relations with a recent experiment are discussed. Section III introduces HBT interference and discusses the classical versus quantum properties of the second-order visibility. A witnessing operator to detect quantum features of this second-order interference is introduced. Quantum properties of two uncorrelated squeezed modes in terms of interference visibility are investigated. In section IV, HBT entanglement witnessing is analyzed for an unsqueezed EPR mixed state. This witnessing operator becomes useful in the discussion of CV Werner states. In Section V we discuss entanglement generated by the action of a beam splitter on two squeezed states. For such general states the properties of the HBT interference are discussed. Finally some conclusions are presented.

II. ONE-MODE GAUSSIAN SQUEEZED STATE

We start our discussion with a brief review of a one-mode GSS of the radiation field. As it is known [15, 16], the most general expression describing the density operator of a GSS characterized by creation and annihilation operators (a, a^\dagger) has the form of a Gaussian operator. Up to linear shifts, this operator can be written in the following normally ordered form

$$\rho = \frac{1}{\sqrt{D}} : \exp \left[-\frac{(n+1)}{D} a^\dagger a - \frac{m}{2D} a^{\dagger 2} - \frac{m^*}{2D} a^2 \right] :, \quad (1)$$

with $D = (n+1)^2 - |m|^2$, where the two parameters, n and $m = |m|e^{i\lambda}$, are related to the following field corre-

*Electronic address: magda.stobinska@fuw.edu.pl

†Electronic address: wodkiew@fuw.edu.pl

lations

$$\langle a^\dagger a \rangle = n, \quad \langle aa \rangle = -m, \quad \langle a^\dagger a^\dagger \rangle = -m^*. \quad (2)$$

In order to represent a physical state ($\rho \geq 0$) these parameters have to satisfy the following inequality

$$|m|^2 \leq n(n+1), \quad (3)$$

where the equality holds only if the density operator is a pure state $\rho = |\Psi\rangle\langle\Psi|$.

Various phase-space distributions, like the Wigner function or the diagonal P -representation of the density operator (1) can be evaluated taking the Fourier transform of the Weyl characteristic function

$$C(\alpha) = \text{Tr}\{D(\alpha)\rho\} = e^{-\frac{1}{2}(\alpha^*, \alpha)\mathbf{C}(\alpha^*)}, \quad (4)$$

where $D(\alpha)$ is the displacement operator, ρ is the density operator given by (1) and

$$\mathbf{C} = \begin{pmatrix} n + \frac{1}{2} & m \\ m^* & n + \frac{1}{2} \end{pmatrix} \quad (5)$$

is the covariance matrix of these Gaussian states.

In general, a positive Gaussian operator is said to be P -representable if there exists its decomposition in a coherent projector basis [17]

$$\rho = \int d^2\alpha P(\alpha)|\alpha\rangle\langle\alpha|, \quad (6)$$

with a non-singular phase-space distribution function $P(\alpha)$. The GSS state given by (1) is P -representable if and only if $n > |m|$, and in this case we have

$$P(\alpha) = \frac{1}{\pi\sqrt{d}} \exp\left[-\frac{n}{d}|\alpha|^2 - \frac{m}{2d}\alpha^{*2} - \frac{m^*}{2d}\alpha^2\right], \quad (7)$$

where $d = n^2 - |m|^2$. This Gaussian distribution with $m = 0$, corresponds to a thermal state with a mean number of photons given by n . A P -representable squeezed Gaussian state can be called classical because its statistical properties can be simulated from the above classical Gaussian distribution function of the field amplitude and phase.

In Fig. 1 we have depicted values of (n, m) for which the mixed Gaussian state is classical (P -representable) or nonclassical (is not P -representable).

Continuous-variable states of light can be described by their electric field amplitude and phase quadratures

$$X_1 = \frac{a + a^\dagger}{\sqrt{2}}, \quad X_2 = \frac{a - a^\dagger}{\sqrt{2}i}, \quad (8)$$

with the commutator $[X_1, X_2] = i$.

The uncertainties of these two quadratures are given by the following relations

$$(\Delta X_1)^2 = \frac{\langle a^\dagger a \rangle + \langle aa^\dagger \rangle + \langle a^2 \rangle + \langle a^{\dagger 2} \rangle}{2}$$

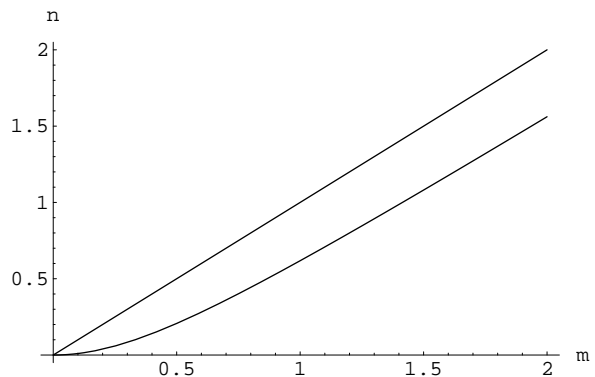


FIG. 1: Quantum and classical one-mode GSS given by (5). According to constraint (3), values on or above the curve specify physical states. Values between the curve and the line describe squeezed, not P -representable, quantum states. P -representable states belong to values on or above the line $n = |m|$.

$$= n + \frac{1}{2} - |m| \cos \lambda, \quad (9)$$

$$\begin{aligned} (\Delta X_2)^2 &= \frac{\langle a^\dagger a \rangle + \langle aa^\dagger \rangle - \langle a^2 \rangle - \langle a^{\dagger 2} \rangle}{2} \\ &= n + \frac{1}{2} + |m| \cos \lambda. \end{aligned} \quad (10)$$

From these uncertainty relations we see that a classical GSS can reduce thermal fluctuations (characterized by the mean number of photons n), to the vacuum level. Quantum GSS can reduce the quantum fluctuations in one quadrature (e.g. amplitude) below the vacuum level at the expense of increased fluctuations in the conjugate variable (phase)

$$(\Delta X_1)^2 < \frac{1}{2}. \quad (11)$$

Such a reduction cannot be described by a P -representable GSS.

As it is well known, the nonclassical nature of GSS can be revealed in a second-order degree of coherence, even though the photon statistics of the vacuum squeezed state is super-Poissonian [17]. For a general mixed GSS, the normalized second-order degree of coherence is

$$g^{(2)} = \frac{\langle a^\dagger a^\dagger aa \rangle}{\langle a^\dagger a \rangle^2} = 2 + \frac{|m|^2}{n^2}, \quad (12)$$

where $g^{(2)} = 3$ is the border value between classical and nonclassical GSS. States, for which $3 \leq g^{(2)} \leq 3 + \frac{1}{n}$, are quantum, so not P -representable. Note that for a small mean number of photons ($n < 1$), $g^{(2)}$ can be very large.

The nonclassical properties of a GSS, can be witnessed using the following quantum witness operator

$$\mathcal{W}^{(2)} = 3 - \frac{a^\dagger a^\dagger aa}{\langle a^\dagger a \rangle^2}. \quad (13)$$

In this case

$$\text{Tr}\{\mathcal{W}^{(2)}\rho\} = \frac{n^2 - |m|^2}{n^2} \quad (14)$$

is positive for P -representable GSS, and negative for not P -representable GSS. Pure state is always quantum, because

$$\langle \Psi | \mathcal{W}^{(2)} | \Psi \rangle = -\frac{1}{n}. \quad (15)$$

A GSS with controllable parameters n and m has been recently generated in an optical parametric amplifier with a phase-insensitive amplifier of gain H followed by a phase-sensitive amplifier of gains G and $1/G$ [18]. In such a generator the incoming mode a_{in} is transformed as follows

$$\begin{aligned} a = & \frac{1}{2} \left(\frac{1}{\sqrt{G}} + \sqrt{G} \right) \sqrt{H} a_{in} + \frac{1}{2} \left(\frac{1}{\sqrt{G}} - \sqrt{G} \right) \sqrt{H} a_{in}^\dagger \\ & + \frac{1}{2} \left(\frac{1}{\sqrt{G}} - \sqrt{G} \right) \sqrt{H-1} v + \frac{1}{2} \left(\frac{1}{\sqrt{G}} + \sqrt{G} \right) \sqrt{H-1} v^\dagger, \end{aligned} \quad (16)$$

where v, v^\dagger are the amplifier quantum noise boson operators. Assuming that modes a_{in} and v are initially empty we obtain that the outgoing state is a GSS with

$$\begin{aligned} n &= \frac{1}{2} \left(\frac{1}{G} + G \right) \left(H - \frac{1}{2} \right) - \frac{1}{2}, \\ |m| &= \frac{1}{2} \left(G - \frac{1}{G} \right) \left(H - \frac{1}{2} \right). \end{aligned} \quad (17)$$

Such a state is P -representable (classical) if $H \geq \frac{1}{2}(G+1)$, and the purity of this state depends only on the phase-insensitive gain $\text{Tr}\{\rho^2\} = \frac{1}{2H-1}$.

Changing the pump average power in the experiment, states with $1 \leq G_{exp} \leq 1.65$ and $1 \leq H_{exp} \leq 1.05$ have been obtained. In this range the GSS was quantum, i.e. not P -representable. For the maximum value of $G_{exp} \simeq 1.65$ and $H_{exp} \simeq 1.05$ the value of H is 20% below the classical threshold. The corresponding value of the normalized second-order degree of coherence, for these gain parameters is purely quantum, $g^{(2)} = 7.68$, with $n \simeq 0.12$ and $|m| \simeq 0.29$, leading to $\text{Tr}\{\mathcal{W}^{(2)}\rho\} = -4.84$, and a purity close to 91%.

III. SECOND-ORDER INTERFERENCE AS A QUANTUM WITNESS

Considering first-order correlation functions and Young-type experiments is not enough to distinguish classical and quantum properties of GSS. Moreover, there is no first-order interference for thermal state at all. It is well known that a second-order interference and Hanbury-Brown and Twiss type experiments [17], can reveal quantum properties of light sources, not seen in Young experiments.

A HBT experiment that we have in mind is depicted on Fig. 2. The source produces two light beams with quantum amplitudes a and b . The interference pattern at the screen is proportional to $1 + v \cos(\varphi_1 - \varphi_2)$, where φ_1 and φ_2 are phase differences between the beams a and b in front of the detectors. These phases include geometrical phases and phases due to the possible action of the beam splitter. The second-order visibility v of these fringes can reveal the quantum nature of the light source. For a classical source the quantum amplitudes of the field are replaced by classical amplitudes and the classical visibility of the fringes v_{cl} is always either equal or less than 50%. This classical limit is violated for single photons, as it has been shown in the pioneering experiments performed by Mandel, reviewed in [19].

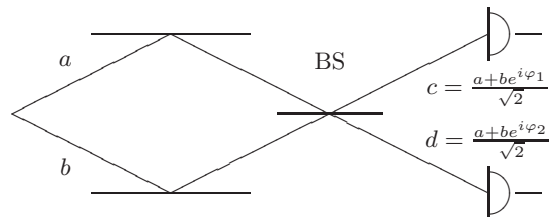


FIG. 2: Hanbury-Brown and Twiss second-order interference.

Let us investigate the HBT interference resulting from two independent GSSs represented by modes (a, b) , for which the density operator is separable (uncorrelated) and has the form

$$\rho = \rho(a) \otimes \rho(b). \quad (18)$$

At the detector the positive-frequency part of electric field (normalized to the number of photons) is as follows

$$E^{(+)}(\varphi_i) = \frac{a + b e^{i\varphi_i}}{\sqrt{2}}. \quad (19)$$

The field intensity operator at the screen is equal to

$$I(\varphi_i) = E^{(-)}(\varphi_i) E^{(+)}(\varphi_i) = \frac{1}{2} (I_a + I_b + b^\dagger a e^{-i\varphi_i} + a^\dagger b e^{i\varphi_i}), \quad (20)$$

where $I_a = a^\dagger a$ and $I_b = b^\dagger b$.

From this expression, we obtain that the normally ordered second-order intensity correlation is

$$\begin{aligned} \langle : I(\varphi_1) I(\varphi_2) : \rangle = & \frac{1}{4} \left[\langle (I_a + I_b)^2 \rangle + 2 \langle I_a I_b \rangle \cos(\varphi_1 - \varphi_2) \right. \\ & + (e^{-i\varphi_1} + e^{-i\varphi_2}) \langle b^\dagger : (I_a + I_b) : a \rangle \\ & + (e^{i\varphi_1} + e^{i\varphi_2}) \langle a^\dagger : (I_a + I_b) : b \rangle \\ & \left. + e^{-i(\varphi_1 + \varphi_2)} \langle b^{\dagger 2} a^2 \rangle + e^{i(\varphi_1 + \varphi_2)} \langle a^{\dagger 2} b^2 \rangle \right]. \end{aligned} \quad (21)$$

If we assume that the two modes have the same mean number of photons $\langle a^\dagger a \rangle = \langle b^\dagger b \rangle = n$ and the squeezing parameters $\langle a^2 \rangle = -m$ and $\langle b^2 \rangle = -m e^{i\lambda}$ differ only by

a phase λ , we obtain the intensity correlation function in the form

$$\langle :I(\varphi_1)I(\varphi_2): \rangle \propto 1 + v_- \cos(\varphi_1 - \varphi_2) + v_+ \cos(\varphi_1 + \varphi_2 + \lambda), \quad (22)$$

where

$$v_- = \frac{2\langle :I_a I_b : \rangle}{\langle : (I_a + I_b)^2 : \rangle}, \quad v_+ = \frac{\langle b^{\dagger 2} a^2 \rangle + \langle a^{\dagger 2} b^2 \rangle}{\langle : (I_a + I_b)^2 : \rangle},$$

$$v_- = \frac{n^2}{3n^2 + |m|^2}, \quad v_+ = \frac{|m|^2}{3n^2 + |m|^2}. \quad (23)$$

In these calculations, normally ordered correlation functions like $\langle a^{\dagger 2} a^2 \rangle$, $\langle a^{\dagger 2} ab \rangle$ and similar, have been evaluated using the Gaussian decomposition of fourth-order correlations into second-order correlations. This follows from the fact that for Gaussian states only second moments are needed to calculate higher moments of the field correlations.

The formulas (21-22), are different from similar formulas involving second-order interference of single photons. Note that the interference pattern consists of two terms being in-phase and out-of-phase $\varphi_1 \mp \varphi_2$. For unsqueezed states the out-of-phase term vanishes.

The interference pattern presented in this equation is genuine to squeezed light. The in-phase visibility v_- appears always, no matter whether the two interfering states are squeezed or not. The out-of-phase visibility v_+ , proportional to $|m|^2$ is entirely due to the squeezing of the incoming modes. If in a realistic experimental situation, the relative phase λ between the two squeezed modes can be controlled, the out-of-phase term contributes to the interference pattern. Note that selecting $\varphi_1 - \varphi_2 = \frac{\pi}{2}$, the interference pattern consists of only out-of-phase fringes proportional to v_+ , and the actual position of the maxima and minima depends on the phase λ .

For an unsqueezed source of light, $|m| = 0$, the interference pattern is thermal with a visibility $v_- = \frac{1}{3}$. At the border line between classical and quantum squeezing, $|m| = n$, the two visibilities are equal $v_- = v_+ = 25\%$. For quantum GSS we always have $v_- \leq v_+$. From these relations we see that the pure GSS is always quantum. Only mixed GSS can reach the classical region. The classical behavior of GSS seen in second-order interference, results in the following set of classical inequalities

$$\frac{1}{4} \leq v_- \leq \frac{1}{3}, \quad 0 \leq v_+ \leq \frac{1}{4}, \quad v_- + v_+ \leq \frac{1}{2}. \quad (24)$$

For quantum sources of GSS, these inequalities are violated, as it is shown in Fig. 3 and Fig. 4, both plotted for two-mode GSS with fixed $n = 1$. The line $m = 1$ is the border between quantum and classical states. The values of m between 1 and $\sqrt{2}$ correspond to quantum GSS, $n < |m|$. The $m = \sqrt{2}$ is the maximal value of this parameter which obeys the positivity constraint $|m|^2 = n(n+1)$. It corresponds to the pure state. The maximum second-order visibility $v = v_- + v_+$ is achieved for angles $\varphi_1 = \varphi_2$ and $\lambda = \varphi_1 + \varphi_2$.

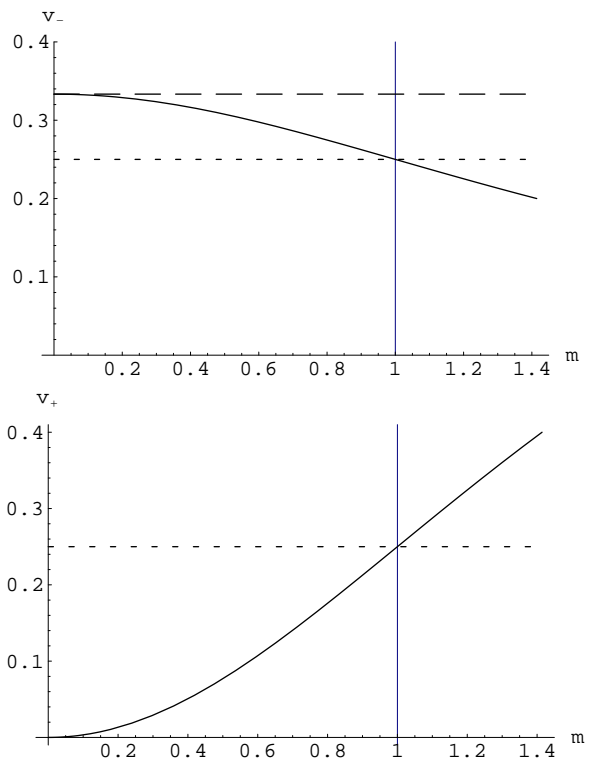


FIG. 3: The visibilities v_- and v_+ (23) evaluated for $n = 1$. The vertical grid line defines a border between classical GSS (values of $|m| < 1$) and quantum GSS ($|m| > 1$). The visibility v_- is always bounded from above by $\frac{1}{3}$ — the dashed horizontal grid line. The dotted grid line, $\frac{1}{4}$, separates the values of v_- and v_+ corresponding to classical and to quantum GSS. v_- is bounded from above and v_+ is bounded from below by $\frac{1}{4}$ for quantum GSS. The value of $|m| = \sqrt{2}$ corresponds to the pure state.

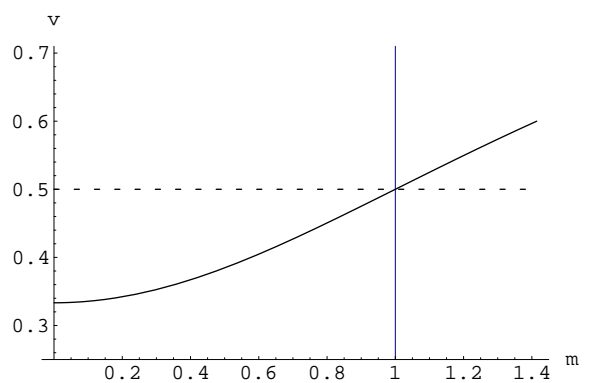


FIG. 4: The sum $v_- + v_+$ evaluated for $n = 1$ is depicted. For quantum GSS ($|m| > 1$ — vertical grid line) the sum is always bounded from below by $\frac{1}{2}$ — horizontal grid line.

We conclude this section, introducing a HBT witness

operator

$$\mathcal{W}^{(HBT)} = \frac{1}{2} - \frac{2a^\dagger b^\dagger ab + b^{\dagger 2} a^2 + a^{\dagger 2} b^2}{\langle (I_a + I_b)^2 \rangle}. \quad (25)$$

For this witness operator we have

$$\text{Tr}\{\mathcal{W}^{(HBT)}\rho\} = \frac{n^2 - |m|^2}{2(3n^2 + |m|^2)}, \quad (26)$$

which is positive for P -representable GSS, and negative for non P -representable GSS.

For the estimated experimental values of the squeezed state discussed in the previous sections, we obtain: $v_- \simeq 11\%$, $v_+ \simeq 66\%$ and $v \simeq 77\%$, resulting with the the value: $\text{Tr}\{\mathcal{W}^{(HBT)}\rho\} \simeq -0.274$, i.e. well below the classical limit.

We will see that the second-order witness (25) can be applied, with some precautions, as an entanglement witness for a correlated squeezed states.

IV. INTERFERENCE WITNESS OF MIXED EPR STATE

Let us investigate a two-mode Gaussian correlated state of Alice and Bob given by a density operator ρ_{AB} . The entangled resource is ideally a two-mode GSS [5] which has annihilation operators a and b . It is well known that such state can be generated in a process of nonlinear optical parametric amplification. For this two-mode Gaussian correlated state the covariance matrix of the Weyl characteristic function, $C(\alpha, \beta) = \text{Tr}\{\rho_{AB}D(\alpha)D(\beta)\}$, is a 4×4 matrix with the following matrix elements

$$\mathbf{C}_{AB} = \begin{pmatrix} n + \frac{1}{2} & 0 & 0 & m_c \\ 0 & n + \frac{1}{2} & m_c^* & 0 \\ 0 & m_c & n + \frac{1}{2} & 0 \\ m_c^* & 0 & 0 & n + \frac{1}{2} \end{pmatrix}, \quad (27)$$

where $\langle a^\dagger a \rangle = \langle b^\dagger b \rangle = n$ and $\langle ab \rangle = -m_c$ is the correlation parameter between the two modes.

In general, in accordance with Werner's separability criterion [20], the two-mode quantum density operator is said to be separable if it is a sum of product states

$$\rho_{AB} = \sum_i p_i \rho^i(a) \otimes \rho^i(b), \quad (28)$$

where $\rho^i(a)$, $\rho^i(b)$ are the density operators of the two modes and $\sum_i p_i = 1$, $p_i > 0$.

As it has been discussed in several papers (see the tutorial [15] and references therein), this two-mode state is the optical analog of the entangled EPR wave function if $|m_c|^2 = n(n+1)$ and $n \rightarrow \infty$. For $n < |m_c|$ the correlated state is entangled, so it is nonseparable and, in general, mixed.

For the mixed EPR state described above the HBT intensity correlation function is a sum of mean values of the following terms

$$\begin{aligned} \langle :I(\varphi_1)I(\varphi_2): \rangle &= \frac{1}{4} \langle a^{\dagger 2} a^2 \rangle + \frac{1}{4} \langle b^{\dagger 2} b^2 \rangle \\ &+ \frac{1}{2} \langle a^\dagger b^\dagger ab \rangle (1 + \cos(\varphi_1 - \varphi_2)), \end{aligned} \quad (29)$$

which can be reduced to

$$\langle :I(\varphi_1)I(\varphi_2): \rangle = \frac{1}{2} (3n^2 + |m_c|^2) (1 + v_- \cos(\varphi_1 - \varphi_2)), \quad (30)$$

where the visibility is

$$v_- = \frac{n^2 + |m_c|^2}{3n^2 + |m_c|^2}. \quad (31)$$

In case of no correlation, i.e. if $|m_c| = 0$, we get $v_- = \frac{1}{3}$ as for a thermal state. For separable states we get $\frac{1}{3} \leq v_- \leq \frac{1}{2}$. For some values of parameters n and m_c the second-order visibility violates the classical limit of $\frac{1}{2}$. For nonseparable, i.e. entangled states, the visibility is always quantum: $v_- > \frac{1}{2}$.

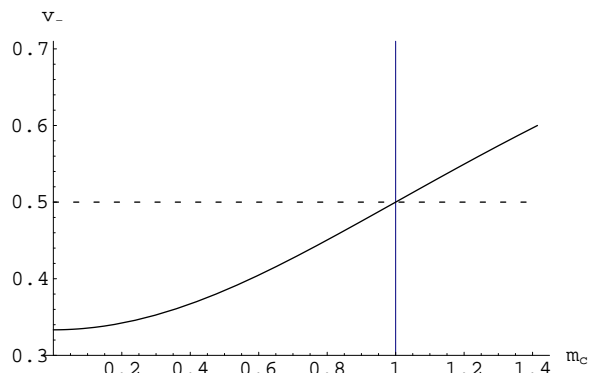


FIG. 5: The visibility v_- (31) of the EPR state. The vertical grid line defines the border between values of $|m_c|$ which correspond to separable and to entangled states. For $|m_c| > 1$ the state is entangled and the visibility is greater than $\frac{1}{2}$ — horizontal grid line.

In Fig. 5 we have depicted this visibility for a mixed EPR states with $n = 1$, as a function of m_c . The range of the correlation parameter, $1 \leq |m_c| \leq \sqrt{2}$, corresponds to mixed nonseparable states, with the exception of the upper boundary, corresponding to a pure state. In this case the maximal visibility is $v_- = 0.6$.

For this mixed two-mode EPR state, we can use the quantum witness operator given by (25) as an entanglement witness. It is easy to see that the last two terms of the witness operator related to single mode squeezing do not contribute and as a result we obtain

$$\text{Tr}\{\mathcal{W}^{(HBT)}\rho_{AB}\} = \frac{n^2 - |m_c|^2}{2(3n^2 + |m_c|^2)}, \quad (32)$$

which is positive for separable mixed EPR states and negative for non separable mixed EPR states.

HBT interference is also useful when detecting entanglement in a Werner-like state. A natural extension of a Werner state for infinite dimensions is a convex combination of a correlated state with the separable maximally mixed states. In this case the Werner state is a combination of a mixed EPR state and two uncorrelated thermal states

$$\rho_W = p\rho_{AB} + (1-p)\rho_A^T \otimes \rho_A^T, \quad (33)$$

where $0 \leq p \leq 1$. The mean number of photons in each mode A and B is the same and equal to n . Simple calculation shows that the visibility of this state is given by

$$v_- = \frac{n^2 + p|m_c|^2}{3n^2 + p|m_c|^2}. \quad (34)$$

From this calculation we see that effectively the Werner state corresponds to a mixed EPR state with correlation parameter m_c scaled by \sqrt{p} . The visibility of this state exceeds 50%, i.e. the entanglement witness (25) turns negative if $n^2 \leq p|m_c|^2$. If the EPR state is a maximally entangled state with $|m_c|^2 = n(n+1)$, this condition simplifies and reads

$$p > \frac{n}{n+1}. \quad (35)$$

For the Werner state with a maximally entangled EPR state, the sufficient criterion for separability involving the positive partial transposition (PPT) can be used and has the form [18]

$$p > \left(1 + \sqrt{\frac{1+n}{n}} \frac{(1+2n^2)^2}{n(1+2n)(1+n^2)} \right)^{-1}. \quad (36)$$

As it is depicted in Fig. 6, the criterion based on the HBT entanglement witness is stronger than the PPT criterion. For the linear combination forming the continuous-variable Werner state given by (33), no proof of the separability condition exists.

V. HBT INTERFERENCE OF ENTANGLED SQUEEZED STATES

The EPR state discussed in the previous section can be generated in a nonlinear optical amplifier. In this section, we discuss entangled two-mode states resulting from a nonlocal operation on two uncorrelated single mode GSSs. This efficient way of producing correlated state uses a beam splitter as the nonlocal operation, that entangles squeezed states of light. A typical setup involves two amplitude squeezed beams, initially separable and shifted in phase, which interfere at the 50/50 beam splitter (Fig. 7).

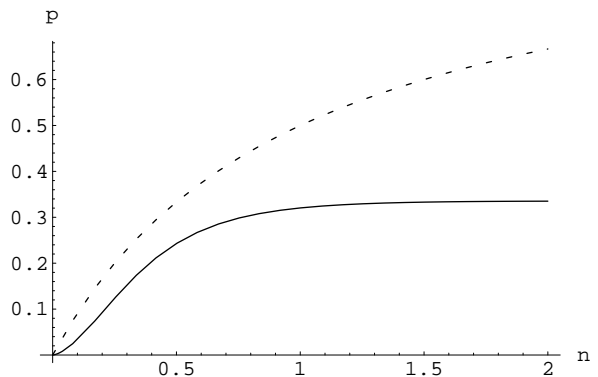


FIG. 6: Comparison of two separability criteria: the dotted line corresponds to HBT interference criterion (35) and the solid line to PPT criterion (36). According to criteria states above the curves are nonseparable.

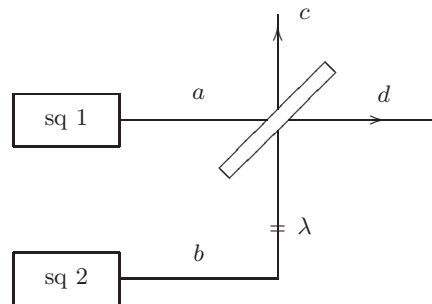


FIG. 7: Schematic experimental setup: two, initially separable, amplitude squeezed beams, shifted in phase (37), interfere at the beam splitter and become entangled. The detectors measure second-order correlation function between modes c and d .

The input squeezed states are characterized by the following parameters

$$\langle a^\dagger a \rangle = \langle b^\dagger b \rangle = n, \quad \langle a^2 \rangle = \langle b^2 \rangle = -m. \quad (37)$$

We recognize in these relations GSSs from Section II. As it is indicated in Fig. 7, the squeezed beam b is shifted by a phase λ .

The relation between input and output modes operators on the beam splitter have the well known form

$$c = \frac{a + be^{i\lambda}}{\sqrt{2}}, \quad d = \frac{a - be^{i\lambda}}{\sqrt{2}}. \quad (38)$$

As a result of this transformation the outcome is also a GSS with the covariance matrix of the modes c and d of the form

$$\mathbf{C}_{out} = \begin{pmatrix} n + \frac{1}{2} & \tilde{m} & 0 & m_c \\ \tilde{m}^* & n + \frac{1}{2} & m_c^* & 0 \\ 0 & m_c & n + \frac{1}{2} & \tilde{m} \\ m_c^* & 0 & \tilde{m}^* & n + \frac{1}{2} \end{pmatrix}. \quad (39)$$

Note that the two output beams form an entangled squeezed EPR state with equal mean number of photons in each mode $\langle c^\dagger c \rangle = \langle d^\dagger d \rangle = n$, equal squeezing parameters in each mode $\langle cc \rangle = \langle dd \rangle = -\tilde{m} = -\frac{1}{2}m(1 + e^{2i\lambda})$ and with correlation parameter $\langle cd \rangle = -m_c = -\frac{1}{2}m(1 - e^{2i\lambda})$. We see the crucial role of the angle λ in the correlation parameter. The correlation parameter m_c is non-zero valued if $\lambda \neq 0, \pi$ and for other values of λ can lead to a state that is nonseparable. For example if $\lambda = \frac{\pi}{2}$ the state (39) reduces to the EPR state (27) with $m_c = m$.

States similar to (39) were produced in [21] using bright beams. In this case the experimental setup consisted of a Sagnac interferometer which produced two independently squeezed beams. In this experimental paper it has been assumed that the output state is a pure unsqueezed EPR state (27).

For the general λ -dependent state, with the tools developed for Gaussian states [15], it is possible to establish the following exact condition for separability

$$|m|^2 + \sqrt{\frac{1 - \cos 2\lambda}{2}} |m| \leq n(n+1), \quad (40)$$

or

$$\sqrt{\left(|m|^2 + \sqrt{\frac{1 - \cos 2\lambda}{2}} |m| + \frac{1}{4} \right)} \leq n. \quad (41)$$

In Fig. 8 we have depicted this condition for three different angles. Note that for incoming not P -representable states, the outcome produced by the beam splitter is never entangled if $\cos 2\lambda = 1$ and is always entangled if $\cos 2\lambda = -1$. As an example, for $\cos 2\lambda = 0$, there are states that are not entangled, despite the quantum nature of the incoming beams. To conclude, it is impossible to produce entangled output from classical input states. For quantum input states, depending on λ , one can produce either entangled or separable state (Fig. 9).

The physical significance of the phase λ is easy to understand when considering the quadratures of the input state. It enables rotation of the error ellipse for a squeezed state in quadrature phase space. Let us consider the quadrature of the input mode $be^{i\lambda}$ rotated by an angle $\frac{\theta}{2}$

$$X_\theta = \frac{be^{i(\lambda - \frac{\theta}{2})} + b^\dagger e^{-i(\lambda - \frac{\theta}{2})}}{\sqrt{2}}. \quad (42)$$

Assuming m to be real for simplicity, its uncertainty is equal to

$$\langle X_\theta^2 \rangle = n + \frac{1}{2} - m \cos(\theta - 2\lambda). \quad (43)$$

The rotated state preserves squeezing of the amplitude (phase) quadrature if $\theta = \pm 2\lambda$, what corresponds to the rotation at an angle $\pm\lambda$. This rotation has a simple geometrical picture of the beam splitter mixing of two independently squeezed states, rotated at different angles,

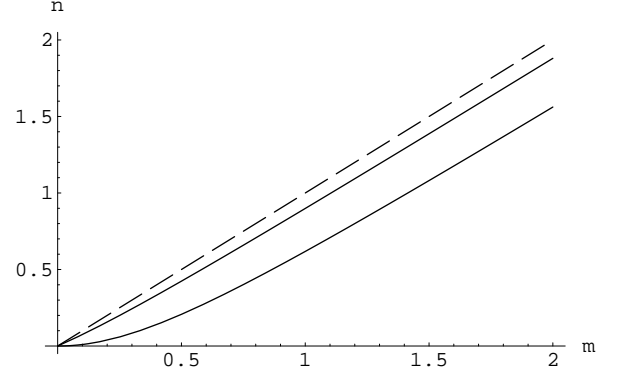


FIG. 8: The constraint (40) for different values of λ is depicted. The line corresponds to $\lambda = \frac{\pi}{2}$ — EPR state (27), the upper curve to $\lambda = \frac{\pi}{4}$ — mixed squeezed EPR state and the lower to $\lambda = 0$ — separable state.

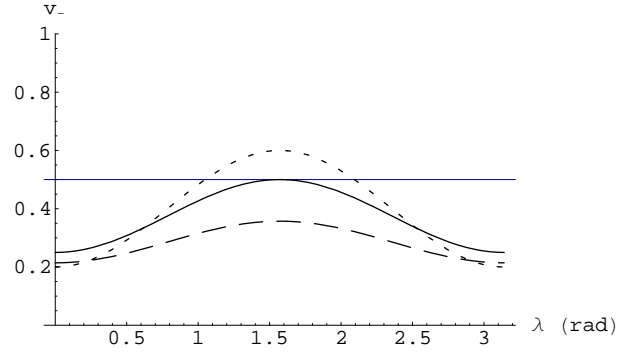


FIG. 9: Depending on the phase λ for the quantum input states, the output state is either of quantum or classical nature. Its v_- , the dotted curve, can exceed $\frac{1}{2}$ — grid horizontal line. For input states with $n = |m|$ the maximum value of v_- for output state is $\frac{1}{2}$, the solid line. Classical input states never give entangled output, the dashed curve never reaches the value of $\frac{1}{2}$.

0 and λ . Such mixing is producing an entangled state since the beam splitter is a nonlocal operation on the two squeezed beams (Fig. 10).

Let us investigate the HBT interference of the state (39). In contrast to the EPR case, the HBT interference leads to phase-dependent in- and out-of-phase visibilities

$$\langle : I(\varphi_1) I(\varphi_2) : \rangle = \frac{1}{2} (3n^2 + |m|^2) [1 + v_- \cos(\varphi_1 - \varphi_2) + v_+ \cos(\varphi_1 + \varphi_2)], \quad (44)$$

$$v_- = \frac{n^2 + \frac{1}{2}(1 - \cos 2\lambda)|m|^2}{3n^2 + |m|^2}, \quad v_+ = \frac{\frac{1}{2}(1 + \cos 2\lambda)|m|^2}{3n^2 + |m|^2}. \quad (45)$$

For these visibilities the set of classical inequalities is

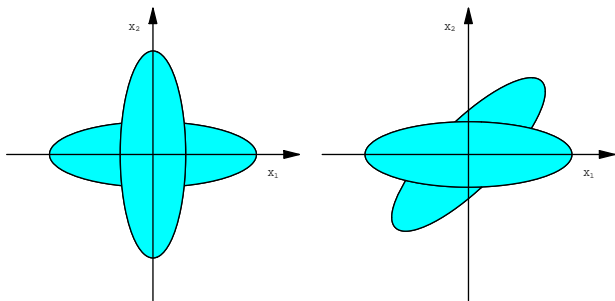


FIG. 10: Beam splitter mixes two independently squeezed states, which error contours are rotated at different angles, and produces an entangled state. For input states rotated at the angles of 0 and $\frac{\pi}{2}$ the outcome is EPR state — left plot. For angles 0 and $\frac{\pi}{4}$ the outcome is a general squeezed state — right plot.

valid

$$\frac{1}{4} \leq v_- \leq \frac{1}{2}, \quad 0 \leq v_+ \leq \frac{1}{4}, \quad v_- + v_+ \leq \frac{1}{2}. \quad (46)$$

Similar inequalities were derived in Sec. III for classical GSS.

This correlation function has been experimentally demonstrated in [22] on Fig.[11], and has been used as an experimental test for the quality of the EPR state. The reduction of noise in the beam, below the vacuum level, was dependent on the value of the mutual phase differences between two squeezed beams, λ .

For input states from the borderline $|m| = n$ between quantum and classical states we have the visibilities, $v_- = \frac{1}{8}(3 - \cos 2\lambda)$ and $v_+ = \frac{1}{8}(1 + \cos 2\lambda)$, that are clearly classical.

In Fig. 11 we have depicted the values of v_- and v_+ for a pure state with mean number of photons $n = 1$ and $|m| = 2$, depending on phase λ . For some angles λ the outcome is entangled, values of its v_- exceed $\frac{1}{2}$ or drops below $\frac{1}{4}$ and values of its v_+ exceed $\frac{1}{4}$.

VI. MORE COMPLICATED CASE

Let us suppose that two modes of correlated Gaussian states investigated in the previous section are not squeezed equally and the two squeezing parameters are not related to the correlation parameter m_c in any way. In such case we can have

$$\begin{aligned} \langle a^\dagger a \rangle &= \langle b^\dagger b \rangle = n, \quad \langle ab \rangle = -m_c, \\ \langle aa \rangle &= -me^{i\lambda_1}, \quad \langle bb \rangle = -me^{i\lambda_2}, \end{aligned} \quad (47)$$

where $\lambda_1 + \lambda_2 \neq \pi$, and m and m_c are real for simplicity. We assume the same mean number of photons n in each mode.

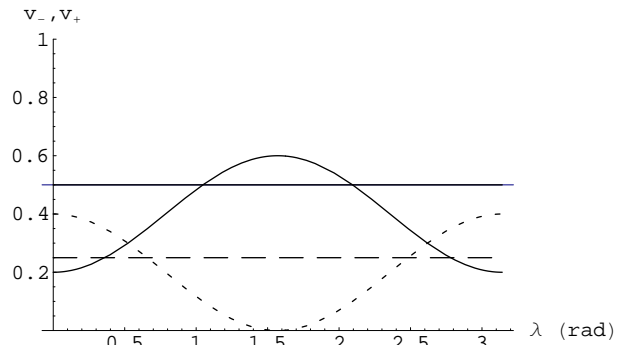


FIG. 11: The values of v_- (the solid curve) and v_+ (the dotted curve) for pure state with $n = 1$ and $|m| = 2$. For some angles λ , values of v_- can exceed $\frac{1}{2}$ (the solid grid line) and values of v_+ can exceed $\frac{1}{4}$ (the dashed grid line). For these angles classical inequalities (46) are violated.

This state is separable if the following separability condition is obeyed

$$m^2 + m_c^2 + |m_c| \sqrt{1 + 2(1 + \cos(\lambda_1 + \lambda_2))m^2} \leq n(n+1). \quad (48)$$

In this case, the in- and out-of-phase terms are not the only terms that can contribute to the second-order interference. Few more cosine terms appear due to the fact that the modes a and b are correlated and these correlations do not cancel when evaluating the expressions $\langle b^\dagger : (I_a + I_b) : a \rangle$ and $\langle a^\dagger : (I_a + I_b) : b \rangle$ (21).

As a result we obtain the following second-order correlation function

$$\begin{aligned} \langle : I(\varphi_1) I(\varphi_2) : \rangle &\propto 1 + v_- \cos(\varphi_1 - \varphi_2) \\ &\quad + v_+ \cos(\varphi_1 + \varphi_2 - \lambda_1 + \lambda_2) \\ &\quad + v_m (\cos(\varphi_1 - \lambda_1) + \cos(\varphi_2 + \lambda_2) \\ &\quad + \cos(\varphi_1 + \lambda_2) + \cos(\varphi_2 - \lambda_1)) \end{aligned}$$

with three visibilities

$$\begin{aligned} v_- &= \frac{n^2 + m_c^2}{3n^2 + m_c^2 + m^2}, \quad v_+ = \frac{m^2}{3n^2 + m_c^2 + m^2}, \\ v_m &= \frac{mm_c}{3n^2 + m_c^2 + m^2}. \end{aligned} \quad (49)$$

The terms modulated by the visibility v_m are genuine to correlated squeezed states.

The appearance of λ_1 and λ_2 in the cosine terms is due to the fact that these two beams are not squeezed equally. In this case they do not give any contribute to the visibilities because the absolute values of squeezing parameters are λ_1 - and λ_2 -independent.

In Fig. 12 visibilities v_- , v_+ , v_m are depicted for a state with a mean number of photons equal to $n = 1$, squeezing parameter $m = \sqrt{2} - m_c$ and phases $\lambda_1 = 0$, $\lambda_2 = \frac{\pi}{2}$. The border value of m_c between separable and

entangled states is equal to $\frac{1}{\sqrt{2}}$. The values of v_- greater than $\frac{3}{8}$ and v_+ less than $\frac{1}{8}$ correspond to entangled states. For v_m the monotonicity decides if the state is entangled.

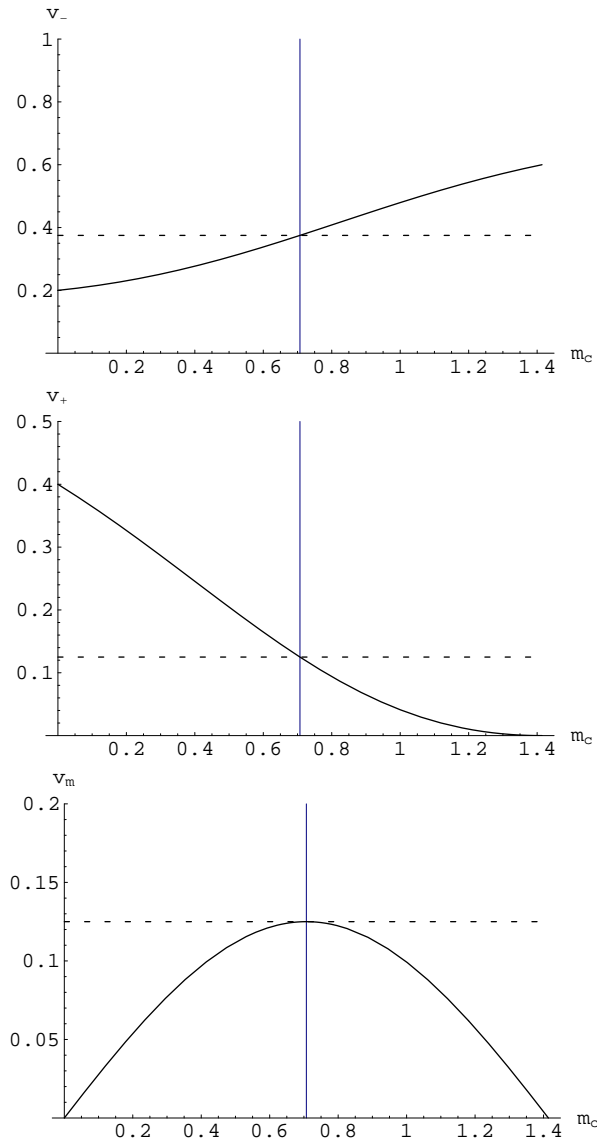


FIG. 12: The visibilities (49) evaluated for $\lambda_1 = 0$, $\lambda_2 = \frac{\pi}{2}$ with $n = 1$ and $m = \sqrt{2} - m_c$. The values of $m_c > \frac{1}{\sqrt{2}}$ — the vertical grid line, correspond to entangled state. $\frac{1}{\sqrt{2}}$ is the maximal value obeying positivity condition. The values of $v_- > \frac{3}{8}$ and $v_+ < \frac{1}{8}$ are genuine to entangled state. Values of v_m are bounded from above by $\frac{1}{8}$.

VII. CONCLUSIONS

In this paper we have presented a new method for witnessing quantum squeezing and entanglement of one- and two-mode mixed Gaussian states. This method relies on HBT interference and second-order intensity correlations. For single mode GSS, a quantum witness operator has been introduced in order to distinguish classical and quantum squeezed states. The quantum features of HBT interference can be probed with the help of HBT witness operator. We have shown that for EPR states this witness operator provides a good test of quantum separability. We have applied the HBT interference and the HBT witness operator to discuss quantum properties of entangled squeezed states generated by a beam splitter. We have shown that the HBT witness operators can be related to second-order visibilities and various classical inequalities.

Acknowledgments

This work was partially supported by a KBN grant No. 2PO3B 02123.

[1] S.L. Branstein and A.K. Pati, (eds), *Quantum Information Theory with Continuous Variable*, (Kulwer, Dordrecht, 2002).

[2] A. Furusawa *et al.*, Science **282**, 706 (1998).

[3] J. Heersink, T. Gaber, S. Lorenz, O. Glöckl, N. Korolkova, and G. Leuchs, Phys. Rev. A **68**, 013815 (2003).

- [4] See for example: B.-G. Englert and K. Wódkiewicz, Phys. Rev. A **65**, 054303-1 (2002), and references therein.
- [5] B.L. Schumaker, Phys. Rep. **135**, 317 (1986).
- [6] Z.Y. Ou, S.F. Pereira, H.J. Kimble, and K.C. Peng, Phys. Rev. Lett. **68**, 3663 (1992).
- [7] B. Yurke, Phys. Rev. A **29**, 408, (1983).
- [8] Ch. Silberhorn, P.K. Lam, O. Weiß, F. König, N. Korolkova, and G. Leuchs, Phys. Rev. Lett. **86**, 4267 (2001).
- [9] N. Korolkova, G. Leuchs, R. Loudon, T. Ralph, and Ch. Silberhorn, Phys. Rev. A **65**, 052306, (2002).
- [10] S. Schmitt, J. Ficker, M. Wolff, F. König, and A. Sizmann, Phys. Rev. Lett. **81**, 2446 (1998).
- [11] L.M. Duan, G. Giedke J.I. Cirac, and P. Zoller, Phys. Rev. Lett. **84**, 2722 (2000).
- [12] R. Simon, Phys. Rev. Lett. **84**, 2726 (2000).
- [13] G. Tóth, C. Simon, and J.I. Cirac, Phys. Rev. A **68**, 062310 (2003).
- [14] M. Horodecki, P. Horodecki, and R. Horodecki, Phys. Lett A **223**, 1 (1996).
- [15] See for example the tutorial: B.-G. Englert and K. Wódkiewicz, International Journal of Quantum Information 1, 153, (2003), and references therein.
- [16] C.W. Gardiner, *Quantum Noise*, (Springer-Verlag, Berlin, 1991).
- [17] See for example: M.O. Scully and M.S. Zubairy, *Quantum Optics*, (Cambridge University Press, Cambridge, UK, 1997).
- [18] J. Wenger, J. Fiurášek, R. Tualle-Broui, N. Cerf, and Ph. Grangier, quant-ph/0403234.
- [19] L. Mandel, Rev. Mod. Phys. **71**, 274, (1999).
- [20] R.F. Werner, Phys. Rev. A **40**, 4277 (1989).
- [21] O. Glöckl, S. Lorenz, C. Marquardt, J. Heersink, M. Brownnutt, Ch. Silberhorn, Q. Pan, P. van Loock, N. Korolkova, and G. Leuchs, Phys. Rev. A **68**, 012319 (2003).
- [22] T.C. Zhang, K.W. Goh, C.W. Chou, P. Lodahl, and H.J. Kimble, Phys. Rev. A **67**, 033802, (2003).